Effect of self-consistency and exchange on the electronic structure of the transition metals, V, Nb, and Ta

L. L. Boyer, D. A. Papaconstantopoulos, and B. M. Klein
Naval Research Laboratory, Washington, D. C. 20375
(Received 10 December 1976)

We have calculated densities of states, Fermi-surface areas, and effective masses from self-consistent augmented-plane wave band-structure calculations for the transition metals vanadium, niobium, and tantalum using the $X\alpha$ exchange approximation. Our results are compared in detail both with the experimental results and the earlier self-consistent and non-self-consistent calculations using other commonly used exchange approximations. We find that the calculated Fermi surfaces are quite sensitive to the exchange approximation used, especially for vanadium. For the self-consistent calculations, there is better overall agreement with the experimental results for the $\alpha = 2/3$ than for the $X\alpha$ calculations. Certain detailed aspects of the experimental Fermi-surface results are discussed and interpreted using the present calculations. We find considerable anisotropy in the electron-phonon mass-enhancement factor obtained from the Fermi-surface results. This anisotropy is found to be very sensitive to the different exchange approximations and to self-consistency.

I. INTRODUCTION

As theories and techniques for calculating band structure continue to improve, one would hope to be able to determine material properties from first principles. For metals it is particularly important to have accurate predictions of Fermi surfaces in order to account quantitatively for such properties as superconductivity and phonon spectra. In this regard the group-VB transition metals, vanadium, niobium, and tantalum are especially interesting because they have high superconducting transition temperatures[1] as well as anomalies in their phonon dispersion curves.[2,3] These metals are also basic building blocks in a host of transition-metal compounds having both theoretical and technological importance.

Because of the importance of the group VB transition metals, we have undertaken a detailed study of their *ab initio* calculated Fermi surfaces and effective masses from potentials constructed using several different exchange approximations in both self-consistent and non-self-consistent calculations.

In Sec. II we describe and catalogue previous experimental and theoretical results on these materials. We describe the new band-structure results and our reworking of some previous calculations in Sec. III. Section IV contains a detailed discussion of the Fermi surfaces from the different calculations and we compare them with the experimental results. In Sec. V we present a discussion of the effective masses and electron-phonon mass-enhancement factors obtained from the Fermi-surface results and relate them to previous calculations using other methods. Finally in Sec. VI we summarize our results.

II. PREVIOUS EXPERIMENTAL AND THEORETICAL WORK

Detailed experimental studies of the Fermi surfaces of the group VB transition metals have been carried out by Halloran *et al.*[4] for Nb and Ta; and by Parker and Halloran[5] for V, using de Haas–van Alphen and magneto-thermal-oscillation measurements. Earlier but less detailed investigations were reported by Phillips[6] for V and Scott *et al.*[7] for Nb.

The calculations of Mattheiss[8] for Nb and Ta, using the non-self-consistent (NSC) augmented-plane-wave (APW) method with the Slater free-electron exchange approximation[9] ($\alpha = 1$), show generally very good agreement with the experimental results. Self-consistent (SC) APW calculations using the Kohn-Sham-Gáspár exchange[10,11] ($\alpha = \frac{2}{3}$) have been performed for V by Papaconstantopoulos *et al.*[12] and for Nb by Anderson *et al.*[13] Their results also agree very well with measured Fermi surface areas for Nb, and they find good, although somewhat less favorable agreement for V. Using a "state dependent" potential and the Korringa-Kohn-Rostoker (KKR) method, Wakoh *et al.*[14,15] similarly obtained good agreement with the measured Fermi surfaces of Nb and V. However, the small number of calculated areas which they report, and the fact that they determine their potential in part by fitting to the measured Fermi surfaces prohibits a meaningful comparison with the results presented here.

Other methods for including exchange, which should in principle be more reliable, are the so-called $X\alpha$ exchange approximation[16] and the Hedin-Lundqvist[17] (HL) modification of the $\alpha = \frac{2}{3}$ exchange. We have performed SC band-structure calculations using the $X\alpha$ method for V, Nb, and Ta. These results are presented and discussed

in Sec. III. We have computed Fermi-surface areas and effective masses from the SC $X\alpha$ band-structure results for comparison with available experimental data and results of earlier calculations. Additional new Fermi-surface results are reported for V obtained from the SC HL potential of Moruzzi *et al.*[18] and from the NSC $\alpha = 1$ potential of Papaconstantopoulos *et al.*[12] Results of the Fermi-surface calculations are discussed in Sec. IV.

Finally we emphasize that all the Fermi-surface calculations that we will discuss are obtained from band structures computed in the muffin-tin approximation. Non-muffin-tin corrections for Nb have been discussed by Painter *et al.*[19] and by Elyashar and Koelling,[20] who find shifts in energy bands of up to 10 mRy for some states.

III. BAND-STRUCTURE RESULTS

We have carried out self-consistent band-structure calculations for V, Nb, and Ta using the $X\alpha$ exchange parameters of Schwarz[16]; namely, $\alpha = 0.715\,56$, $0.703\,83$, and $0.693\,19$ for V, Nb, and Ta, respectively. Spin-independent relativistic effects were included for Ta.[21] The computational procedure used for obtaining self-consistency is discussed in Refs. 12 and 13. In addition we use a method which permits a relaxation of both core and valence states in the iteration process. The charge density of the deep core states is computed atomiclike in each iteration, while some of the higher "semicore" states, as well as the valence states are treated as bands. These semicore states are ns and np, where $n = 3$, 4, and 5 for V, Nb, and Ta, respectively. For Ta the $4f$ semicore states were also treated as bands.

Results for the band structure of Ta are shown in Fig. 1. We find no significant qualitative differences between these results and the NSC $\alpha = 1$ results of Mattheiss.

Density of states (DOS) for all three metals are shown in Figs. 2–4. For comparison in Figs. 5 and 6 we show the DOS of V and Nb obtained from the SC $\alpha = \frac{2}{3}$ potentials of Refs. 12 and 13. In all cases the DOS were calculated from a sum over 274 400 random $\vec{k}$ points using a Slater-Koster[32] interpolation scheme in which the parameters (listed in Appendix A) were determined by least-squares fitting to ~200 first-principles APW energy values. In order to speed up the DOS calculation, the Slater-Koster energies were fitted using the QUAD method[23] on a very large mesh of 1240 $\vec{k}$ points in the $\frac{1}{48}$ Brillouin zone. The results in Figs. 5 and 6 are more accurate than those published previously[12,13] owing to the better interpolation method. From the Slater-Koster method

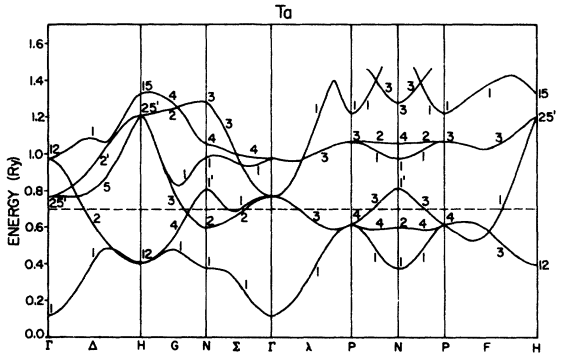

FIG. 1. Self-consistent energy bands for Ta in the $X\alpha$ exchange approximation.

a decomposition of the DOS into s, p, $d_{\Gamma_{25}'}$, and $d_{\Gamma_{12}}$ character is possible. These decomposed DOS are also shown in Figs. 2–6.

While the qualitative features between the $X\alpha$ and the $\alpha = \frac{2}{3}$ results are quite similar, there are some appreciable quantitative differences. This is illustrated in Table I where the DOS values at the Fermi level are tabulated.

IV. FERMI-SURFACE RESULTS

A. Comparison of Fermi surfaces from different potentials

The Fermi-surface areas and effective masses were determined using two separate interpolation

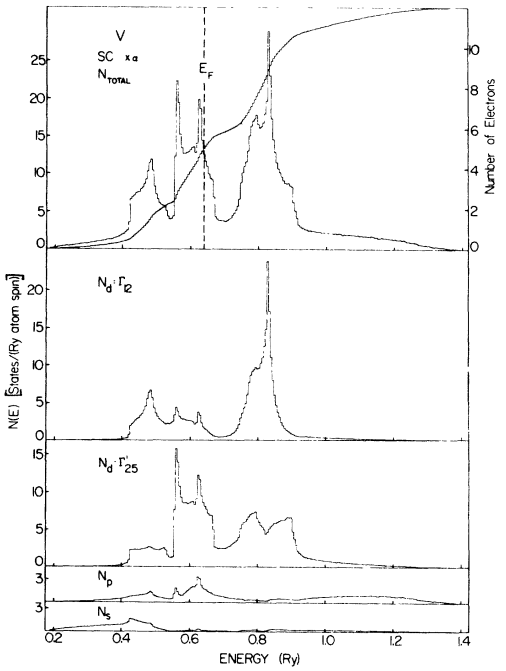

FIG. 2. Total and decomposed densities of states from the self-consistent energy bands of V using the $X\alpha$ exchange approximation.

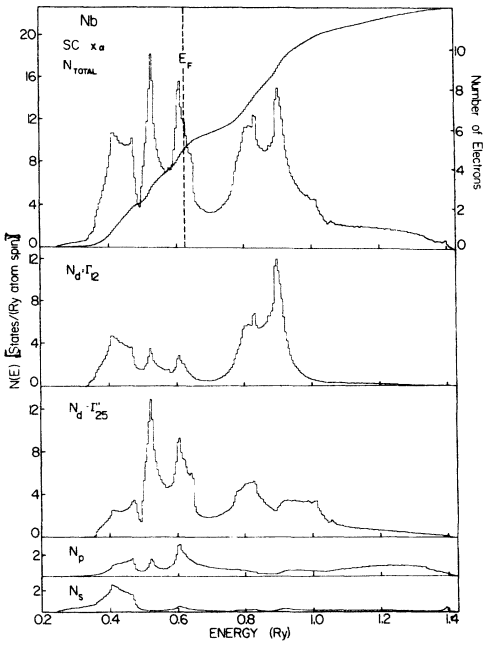

FIG. 3. Total and decomposed densities of states from the self-consistent energy bands of Nb using the $X\alpha$ exchange approximation.

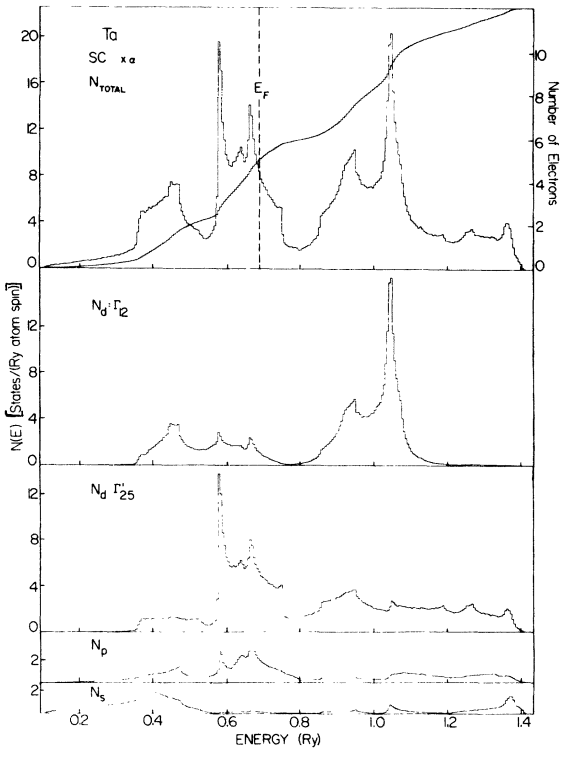

FIG. 4. Total and decomposed densities of states from the self-consistent energy bands of Ta using the $X\alpha$ exchange approximation.

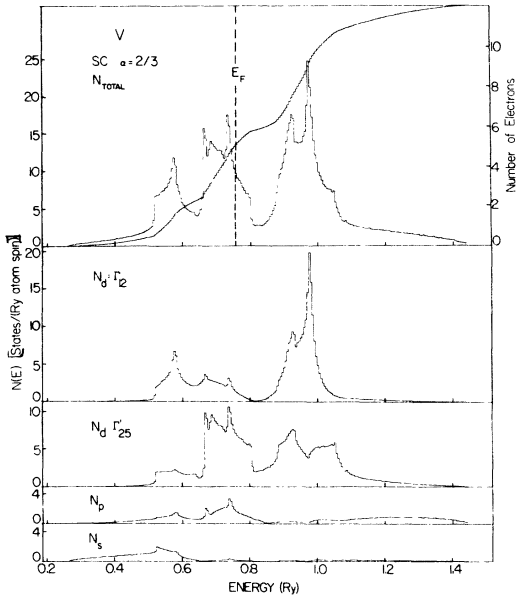

FIG. 5. Total and decomposed densities of states from the self-consistent energy bands of V using the $\alpha=\frac{2}{3}$ exchange approximation.

formulas for the band energies $E_n(\vec{k})$: (i) a QUAD fit[23] of the $n=2$ and $n=3$ bands, i.e., those bands which cross the Fermi energy, to the first-principle values at 285 $\vec{k}$ points in the $\frac{1}{48}$ irreducible Brillouin zone; and (ii) the Slater-Koster scheme described in Sec. III and in Appendix A. The QUAD interpolation gave $\lesssim 3$ mRy rms fitting error in all cases, while the Slater-Koster errors were somewhat larger, with 4- and 7-mRy rms errors for V and Nb, respectively. Although the Slater-Koster scheme has a larger rms error, it is worth noting that only 200 first-principles energies from six bands were fitted, while in the QUAD scheme we fitted 285 energies per band. Once $E_n(\vec{k})$ is available in an efficient form it is a straightforward matter to determine the extremal areas and associated effective masses.

Results obtained from our self-consistent $X\alpha$ band structures are listed in Tables II–IV for V, Nb, and Ta along with the experimental values and the results of other calculations. The various orbits are labeled according to the convention of Mattheiss.[8] Based on a comparison of the Fermi surfaces obtained from the QUAD and Slater-Koster formulas for $E_n(k)$, we conclude that the calculated areas reported here are accurate to ~6% while the effective masses are accurate to ~15%, due to possible inaccuracies in the band energy fits. The SC $\alpha=\frac{2}{3}$ results, which differ slightly from those published previously, were obtained from the

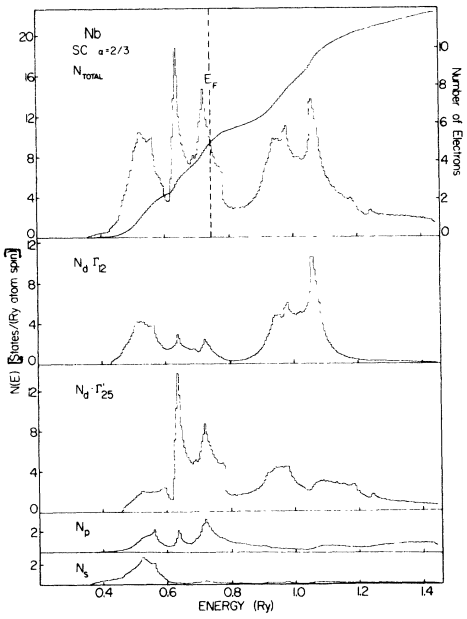

FIG. 6. Total and decomposed densities of states from the self-consistent energy bands of Nb using the $\alpha=\frac{2}{3}$ exchange approximation.

Slater-Koster fit and should be more reliable than the earlier values (obtained by graphical interpolation). Also shown in Table II are results obtained from two additional vanadium potentials: (i) a NSC $\alpha=1$ potential obtained using the $(3d)^4(4s)^1$ atomic configuration; and (ii) the potential of

TABLE I. Total and decomposed DOS at the Fermi level from SC $X\alpha$ and SC $\alpha=\frac{2}{3}$ calculations.

		$N(E_F)$ [states/(atom Ry spin)]				
		Total	s	p	$d_{\Gamma_{25}'}$	$d_{\Gamma_{12}}$
V	$X\alpha$	12.380	0.162	1.893	8.628	1.697
	$\alpha=\frac{2}{3}$	10.073	0.134	1.616	7.023	1.300
Nb	$X\alpha$	10.514	0.342	1.868	6.601	1.703
	$\alpha=\frac{2}{3}$	8.983	0.200	1.929	5.609	1.245
Ta	$X\alpha$	7.980	0.129	1.834	4.959	1.058

Moruzzi *et al.*[18] which was obtained from a SC Korringa-Kohn-Rostoker calculation in which the Hedin-Lundqvist[17] modification of the $\alpha=\frac{2}{3}$ exchange was used.

For Nb and V the SC $X\alpha$ results have significantly worse agreement with the experimentally determined Fermi surface than either the NSC $\alpha=1$ or the SC $\alpha=\frac{2}{3}$ results. Both the NSC $\alpha=1$, and the SC $\alpha=\frac{2}{3}$ results agree very well with the measured values for Nb; while the agreement is good for V, although somewhat worse than for Nb. On the other hand for Ta, both the SC $X\alpha$ and the NSC $\alpha=1$ results agree well with the experimental Fermi surface. This is not inconsistent with the trend from Nb to V because: (i) the value of α in the $X\alpha$ approximation is closer to $\frac{2}{3}$ for the heavier elements; and (ii) the results seem to be less sensitive to the exchange approximation as Z, the atomic number, increases (compare the results in

TABEL II. Calculated and measured Fermi-surface areas and effective masses for selected extremal orbits of vanadium.

		Areas (nm^{-2})				Effective masses			m^*/m_0	
Orbit[a]	Expt.[b]	SC $\alpha=\frac{2}{3}$[c]	SC $X\alpha$	NSC $\alpha=1$[c]	SC HL[d]	Expt.[b]	SC $\alpha=\frac{2}{3}$[c]	SC $X\alpha$	NSC $\alpha=1$[c]	SC HL[d]
[001]JG(Δ)	28	42	34	40	31	3.2	1.30	1.45	1.39	1.59
$E(1,2)$	50.5	40	65	44	64	1.77	0.72	1.39	0.78	1.45
$E(3,4,5,6)$	57.6	54	76	58	76	2.08	0.93	1.14	1.00	1.14
JG(N)		131	149	134	144		1.84	3.13	2.00	3.01
OCT		189	151	186	158		2.50	2.63	2.89	2.90
[111] $E(1,3,4)$	47.9	46	61	50	59	1.77	0.77	0.90	0.84	0.89
$E(2,5,6)$		49	80	53	78		0.90	1.52	0.97	1.52
OCT		132	85	123	91		2.64	2.85	2.82	2.89
JG(Γ)		150	133	145	138		2.83	3.86	3.04	3.53
JG(H)		266	238	268	242		2.31	2.06	2.56	2.20
[110] $E(1)$	53.2	53	70	58	68	2.20	0.88	0.81	0.92	0.87
$E(2)$	64.1	54	86	57	85		0.91	1.34	0.94	1.37
$E(3,4,5,6)$	50.7	45	65	49	63	1.72	0.77	1.02	0.83	1.03
OCT		152	117	147	122		2.30	2.82	2.44	2.78

[a] Notation of Ref. 8, JG: jungle gym. OCT: octahedron. $E(1),\ldots,E(6)$: ellipsoids.
[b] Reference 5.
[c] From potential of Ref. 12.
[d] From potential of Ref. 18 with exchange treated as in Ref. 17.

TABLE III. Calculated and measured Fermi-surface areas and effective masses for selected extremal orbits of niobium.

Orbit[a]	Areas (nm^{-2}) Expt.[b]	SC $\alpha=\frac{2}{3}$[c]	SC $X\alpha$	NSC $\alpha=1$[d]	Effective masses m^*/m_0 Expt.[b]	SC $\alpha=\frac{2}{3}$[c]	SC $X\alpha$	NSC $\alpha=1$[d]
[001]JG(Δ)	13.8	16	12	11.7	1.12	0.53	0.62	0.57
$E(1,2)$	63.0	64	71	64.2		0.70	0.86	0.83
$E(3,4,4,6)$	81.5	82	97	85.5	1.60	0.79	1.06	0.97
JG(N)		143	157	149.4		1.47	2.06	1.74
OCT		115	80	88.1		1.81	1.89	1.92
[111]$E(1,3,4)$	64.7	64	74	66.3	1.28	0.57	0.92	0.73
$E(2,5,6)$	81.0	78	98	86.7		0.82	1.18	1.12
OCT		61	36	45.3		1.16	1.17	1.54
JG(Γ)		99	68	74.2		2.09	2.66	2.29
JG(H)	186.2	183	179	188.1		1.07	1.02	1.17
[110]$E(1)$	76.0	75	83	76.2		0.69	0.79	0.79
$E(2)$	85.7	86	104	94.0		0.83	1.08	0.98
$E(3,4,5,6)$	64.7	66	75	67.7	1.22	0.60	0.74	0.70
OCT		89	57	67.5		1.71	1.74	1.66

[a] Notation of Ref. 8.
[b] Reference 4.
[c] From potential of Ref. 13.
[d] Reference 8.

Tables II and III).

We also note that the SC $X\alpha$ and the SC local density scheme[17] determined Fermi-surface areas are almost identical for V. This agrees with the general observation of Williams *et al.*[24] that SC band structures performed for both the $X\alpha$ and the HL local density exchange approximations give nearly equivalent energy bands. This is related to the fact that the average α in the HL local density approximation is very close to the $X\alpha$ value.[24]

The NSC calculations using the full Slater exchange ($\alpha=1$) and an atomic configuration for the valence-conduction states of one s electron for V and Nb, and two s electrons for Ta also give good agreement with the measured Fermi surface. However, especially for Nb where both the NSC $\alpha=1$ and the SC $\alpha=\frac{2}{3}$ results agree very well with experiment, there are very significant differences for calculated surface areas which have not been measured. Specifically, the two calculations differ by ~25% for the second zone ($n=2$, octahedron) extremal areas, with similar sized discrepancies for the jungle-gym (JG) surface at Γ.

The NSC $\alpha=1$ results of Elyashar and Koelling[20] for Nb show that relativistic and non-muffin-tin corrections to the Fermi surface are significant and tend to spoil the good agreement with experiment obtained by Mattheiss.[8] However, the changes are generally smaller than what we find in our SC calculations upon changing the exchange from $\alpha=\frac{2}{3}$ to $X\alpha$. Their most recent results, which include self-consistency, relativistic, and non-muffin-tin effects, support our conclusion that the SC $\alpha=\frac{2}{3}$ potential gives better agreement with experimental results than does SC $X\alpha$.

B. Some more subtle features of the Fermi surfaces

We find some rather sharp features in the shape of the JG Fermi surfaces which are not evident from the figures shown in Ref. 8. This is illus-

TABLE IV. Calculated and measured Fermi-surface areas and effective masses for selected extremal orbits of tantalum.

Orbit[a]	Area (nm^{-2}) Expt.[b]	SC $X\alpha$	NSC $\alpha=1$[c]	Effective masses m^*/m_0 Expt.[b]	SC $X\alpha$	NSC $\alpha=1$[c]
[001]JG(Δ)	27.9	31	29.2	1.35	0.82	0.84
$E(1,2)$	43.6	39	39.5	1.09	0.69	0.60
$E(3,4,5,6)$	58.5	58	56.7		0.79	0.78
JG(N)		115	114.7		1.31	1.31
OCT		138	132.4		1.77	1.66
[111]$E(1,3,4)$	47.2	45	44.8	1.06	0.61	0.60
$E(2,5,6)$	55.0	53	52.0		0.83	0.81
OCT		97	90.0		1.55	1.68
JG(Γ)		117	113.0		0.96	1.94
JG(H)	197.6	200	198.8		1.28	1.43
[110]$E(1)$	58.0	58	56.2	1.35	0.71	0.61
$E(2)$		60	58.0		0.82	0.75
$E(3,4,5,6)$	47.2	45	44.2	1.18	0.63	0.80
OCT		113	106.5		1.24	1.46

[a] Notation of Ref. 8.
[b] Reference 4.
[c] Reference 8.

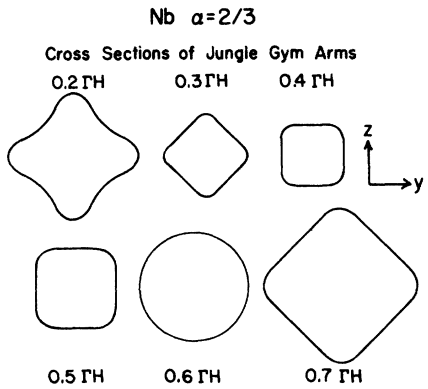

FIG. 7. Shape of the jungle-gym Fermi surface, for Nb (SC $\alpha=\frac{2}{3}$), in the planes $x=0.2,\ 0.3,\ \ldots,\ 0.7$ of the way from Γ to H.

trated in our Fig. 7 for the Nb SC $\alpha=\frac{2}{3}$ results where six cross sections of the JG arms, in particular the closed lines on the Fermi surface in the $x=0.2, 0.3, \ldots, 0.7$ planes (Γ to H distance identical to 1), are shown. Results for the other materials and other exchanges show similar features. Near the center between Γ and H ($x\sim0.5$), the cross sections are nearly square, with sides parallel to the y and z directions. Moving toward Γ or H, the cross sections become nearly circular at a point between 0.3 and 0.4, and at ~0.6. At 0.3 and 0.7 the shape is again nearly square, but here the figures are rotated by 45°, i.e., the sides are parallel to the (0, 1, 1,), (0, −1, 1), (0, 1, −1), and (0, −1, −1) directions. Moving yet closer to Γ or H, the corners become elongated and quickly open up into the other JG arms parallel to the y and z directions.

Owing to these sharp changes in shape of the JG arms, one should not be surprised to find some additional extremal areas which correspond with some of the additional observed frequencies. We looked carefully at a number of angles for additional extremal areas along the JG arms of the Nb $\alpha=\frac{2}{3}$ Fermi surface without success. However, it may be that structure on such a fine scale is present, but is washed out by the interpolation scheme.

We do find noncentral extremal orbits associated with the JG (H) surface of Ta of the kind anticipated and discussed by Halloran *et al.*[4] Specifically, for a field direction of 35° from ⟨100⟩ (see Fig. 5 of Ref. 4) we find a central maximal orbit of 243 nm^{-2} and a noncentral minimal orbit of 233 nm^{-2}. As the field direction angle increases, the area of the noncentral orbit decreases more slowly than that of the central orbit, so that beyond ~40° the only extremal orbit is the central one which is now a minimal orbit.

The measurements of Parker and Halloran[5] on vanadium tend to support the existence of narrow "necks" which join the "ellipsoids" to the JG surface along the ΓN direction. The existence of such necks implies that the third band along the Σ direction does *not* cross the Fermi level. Our results have this band dipping below the Fermi level by the amounts 16, 4, 6, 14, and 18 mRy for Ta $X\alpha$, Nb $X\alpha$, Nb $\alpha=\frac{2}{3}$, V $X\alpha$, and V $\alpha=\frac{2}{3}$, respectively. Thus our calculations indicate in all cases that such necks do not exist. Furthermore there is no trend which would indicate that their existence would be more likely in V than in Nb or Ta. To the contrary, the calculations suggest a greater likelihood for their existence in Nb rather than V or Ta. However, there is no experimental evidence for the existence of these necks in Nb.

In all our calculations, we find that the general shape of the second-zone "octahedral" surface is strikingly different for Nb than for V or Ta. Specifically the shape of the protrusions along the [100] directions are much more elongated for Nb, giving a picture which more nearly resembles a jack than an octahedron. In fact, the SC $X\alpha$ results for Nb show two additional extremal orbits on the arms of the "jack" with areas of ~8 and 10 nm^{-2}. Elyashar and Koelling[20] also find similar extra orbits only when they include non-muffin-tin corrections in their NSC $\alpha=1$ calculations for Nb. However, we believe that this is likely not the correct explanation of the additional α branches observed by Halloran *et al.*[4] because: (i) a similar explanation is not possible for the same kind of signals observed in V (see Ref. 5) owing to the nearly octahedral shape of the second-zone surface of V; and (ii) the SC $\alpha=\frac{2}{3}$ results, which give the best overall agreement with the experimental results, do not show these extra orbits.

V. ELECTRON-PHONON MASS ENHANCEMENT

For each calculated Fermi-surface orbit, the band-structure effective masses shown in Tables II–IV were determined numerically from the formula

$$\left(\frac{m^*}{m_0}\right)_{\text{band}}=\frac{1}{\pi}\left(\frac{\partial A_{\text{band}}}{\partial E}\right)_{E_F}, \tag{1}$$

in atomic units with A the area and E the energy.

The experimentally measured effective mass is, however, enhanced by the electron-phonon interaction, so that

$$\left(\frac{m^*}{m_0}\right)_{\text{measured}}=\left(\frac{m^*}{m_0}\right)_{\text{band}}(1+\lambda_{\text{orb}}), \tag{2}$$

where for each particular orbit, λ_{orb}, defined by

TABLE V. Electron-phonon mass-enhancement factors obtained from the Fermi-surface results in Tables II–IV (λ_{orb}), for comparison with values obtained from McMillian's equation (λ_{emp}) and results of first-principles calculations (I and II of Ref. 26).

	V SC $X\alpha$	V SC $\alpha=\frac{2}{3}$	V SC HL	V NSC $\alpha=1$	Nb SC $X\alpha$	Nb SC $\alpha=\frac{2}{3}$	Nb NSC $\alpha=1$	Ta SC $X\alpha$	Ta NSC $\alpha=1$
λ_{orb} [001]JG(Δ)	1.21	1.46	1.01	1.30	0.81	1.11	0.96	0.65	0.61
[001] $E(1,2)$	0.27	1.46	0.22	1.27	...	...	...	0.58	0.82
[001] $E(3,4,5,6)$	0.82	1.24	0.82	1.08	0.51	1.03	0.65	...	...
[111] $E(1,3,4)$	0.97	1.30	0.99	1.11	0.39	1.25	0.75	0.74	0.77
[110] $E(1)$	1.72	1.50	1.53	1.39	...	...	...	0.90	0.93
[110] $E(3,4,5,6)$	0.69	1.23	0.67	1.07	0.65	1.03	0.74	0.87	0.80
$\bar{\lambda}_{orb}$	0.95±0.45	1.37±0.11	0.87±0.39	1.20±0.12	0.59±0.16	1.11±0.09	0.78±0.1	0.75±0.12	0.79±0.10
λ_{emp}	0.67	0.67	0.67	0.67	0.94	0.94	0.94	0.74	0.74
λ_I	1.35	1.43	1.34	1.30	1.34	1.39	...	0.98	...
λ_{II}	0.69	...	...	...	0.99	...	...	0.87	...

Eq. (2), is the electron-phonon mass-enhancement factor averaged over the particular orbit.

In Table V we show the values of λ_{orb} that we have obtained using our results shown in Tables II–IV. We also show the values of $\bar{\lambda}_{orb}$ which are simple arithmetic averages of the various λ_{orb}; and λ_{emp} which is the empirical value obtained by inverting the McMillan[25] equation for the superconducting transition temperature T_c with $\mu^* = 0.13$.

We also show in Table V the quantities λ_I and λ_{II} obtained from our first-principles calculations[26] using the theory of Gaspari and Gyorffy.[27] This theory is based on the motion of rigid-muffin-tin potentials and contains an implicit average over the Fermi surface. The differences between λ_I and λ_{II} result from technical problems related to the rigid-muffin-tin approximation (see Ref. 26 for a full discussion).

We see from Table V that there is, in general, considerable quantitative differences between the different λ values, although in all cases the materials are predicted to be good superconductors. It is to be noted however, that the values of $\bar{\lambda}_{orb}$ are averages over a relatively small number of orbits, so that it is not clear what kind of accuracy to expect from these values (the rms deviations from the averages are shown following these numbers). In this regard note that the values of λ_I show very little variation with exchange for a given material, while the $\bar{\lambda}_{orb}$ are much more rapidly varying. It appears that the values of λ computed from the Gaspari-Gyorffy theory, which are implicit averages over the *whole* Fermi surface, are not very exchange sensitive, showing very weak dependence on the "detailed" shape of the Fermi-surface pieces. However, since there is current interest in discussing anisotropies in quantities such as λ and the superconducting energy-gap function[28]—quantities similar to our λ_{orb} values—it should be noted that there is a very large variation in the values of λ_{orb} for the different ways of constructing potentials. This point must be given careful consideration in any detailed anisotropy studies.

VI. CONCLUSIONS

We have presented detailed calculations of the Fermi surfaces and the densities of states of the transition metals vanadium, niobium, and tantalum. In general, we find that the Fermi-surface areas are extremely sensitive to the exchange parameter α, with this becoming less of a factor with increasing atomic number. The SC calculations employing the $\alpha=\frac{2}{3}$ exchange give significantly better agreement with the experimen-

TABLE VI. Slater-Koster energy integrals E and resultant rms errors, both in Ry. The notation can be related to that of Ref. 22 if the indices 1–9 are replaced by the symbols: s, x, y, z, xy, yz, xz, x^2-y^2, and $3z^2-r^2$.

	Vanadium		Niobium		Tantalum
	$\alpha=0.7156$	$\alpha=\frac{2}{3}$	$\alpha=0.7038$	$\alpha=\frac{2}{3}$	$\alpha=0.6932$
$E_{11}(000)$	1.1279	1.2271	1.1719	1.3144	0.9962
$E_{11}(111)$	−0.0869	−0.0885	−0.0714	−0.0700	−0.0850
$E_{12}(111)$	−0.0434	−0.0614	−0.0606	−0.0561	−0.0619
$E_{15}(111)$	0.0413	0.0445	0.0563	0.0590	0.0577
$E_{22}(000)$	1.2515	1.5082	1.4276	1.4765	1.4173
$E_{22}(111)$	−0.0185	0.0243	0.0282	0.0153	0.0309
$E_{23}(111)$	0.0472	0.0551	0.0478	0.0412	0.0448
$E_{25}(111)$	0.0215	0.0281	0.0395	0.0441	0.0477
$E_{26}(111)$	0.0379	0.0417	0.0471	0.0525	0.0558
$E_{28}(111)$	0.0217	0.0161	0.0189	0.0200	0.0195
$E_{55}(000)$	0.7490	0.8937	0.7908	0.9541	0.9461
$E_{55}(111)$	−0.0142	−0.0154	−0.0228	−0.0254	−0.0275
$E_{57}(111)$	−0.0228	−0.0252	−0.0352	−0.0392	−0.0432
$E_{59}(111)$	0.0174	0.0172	0.0195	0.0186	0.0216
$E_{99}(000)$	0.7212	0.8559	0.7362	0.8788	0.8617
$E_{99}(111)$	0.0237	0.0265	0.0306	0.0337	0.0357
$E_{11}(200)$	−0.0869	−0.0584	−0.0549	−0.0580	−0.0352
$E_{12}(200)$	−0.0683	−0.0770	−0.0766	−0.0884	−0.0703
$E_{19}(002)$	−0.0291	−0.0402	−0.0398	−0.0530	−0.0450
$E_{22}(200)$	0.0529	0.1097	0.1046	0.1108	0.1287
$E_{33}(200)$	−0.0266	−0.0116	−0.0165	−0.0333	−0.0231
$E_{25}(020)$	−0.0099	−0.0066	−0.0103	−0.0138	−0.0104
$E_{49}(002)$	−0.0413	−0.0639	−0.0692	−0.0792	−0.0803
$E_{55}(200)$	0.0097	0.0098	0.0069	0.0038	0.0033
$E_{55}(002)$	0.0009	0.0015	0.0050	0.0096	0.0090
$E_{99}(002)$	−0.0384	−0.0441	−0.0561	−0.0656	−0.0705
$E_{88}(002)$	0.0017	0.0028	0.0034	0.0057	0.0072
$E_{11}(220)$	0.0232	0.0082	−0.0017	−0.0038	0.0003
$E_{12}(220)$	0.0142	0.0067	0.0016	0.0036	0.0037
$E_{15}(220)$	−0.0039	−0.0035	0.0002	−0.0035	−0.0034
$E_{19}(220)$	−0.0001	0.0008	0.0003	−0.0051	−0.0050
rms Error	0.0045	0.0047	0.0075	0.0090	0.0090

tal results than does the $X\alpha$ exchange or the local density exchange of Hedin and Lundqvist. The HL and the $X\alpha$ exchange yields nearly identical Fermi surfaces, as noted earlier by Williams *et al.*[24] Non-self-consistent calculations with $\alpha=1$ give good agreement with experimental results, similar to the SC $\alpha=\frac{2}{3}$ calculations, although there are significant differences in the results of the two calculations for orbits which have not been measured. We have also found that the electron-phonon mass-enhancement factor λ calculated from the orbital effective masses exhibits considerable anisotropy over the Fermi surface. It is also very sensitive to the exchange approximation, and agrees on the average, qualitatively, with the value calculated using the Gaspari-Gyorffy theory.

ACKNOWLEDGMENTS

We are grateful to A. R. Williams, V. L. Moruzzi, and J. F. Janak for helpful discussions and for providing us with their potentials, and to D. D. Koelling for discussions and preliminary reports of unpublished work. We also wish to thank L. S. Birks and D. J. Nagel for a critical reading of the manuscript, J. W. McCaffrey for assistance with the band calculations, and G. Kamm for helpful discussions of the Fermi surfaces of transition metals.

APPENDIX A

Our Slater-Koster interpolation scheme uses the 27 parameters corresponding to the interaction in-

tegrals of the first and second nearest neighbors plus four additional parameters representing the third neighbor s-s, s-p, and s-d interactions. These 31 parameters are given in Table VI for all our calculations. Our notation can be related to that of the original Slater and Koster paper if the indices 1–9 are replaced by the symbols: s, x, y, z, xy, yz, zx, x^2-y^2, and $3z^2-r^2$. The final row of Table VI gives the rms deviation of the Slater-Koster energies from the first-principles values corresponding to a mesh with 55 k points in the $\frac{1}{48}$ Brillouin zone.

[1]B. T. Matthias, T. H. Geballe, and V. B. Compton, Rev. Mod. Phys. 35, 1 (1963).

[2]Y. Nakagava and A. D. B. Woods, Phys. Rev. Lett. 11, 271 (1963).

[3]A. D. B. Woods, Phys. Rev. 136, A781 (1964).

[4]M. H. Halloran, J. H. Condon, J. E. Graebner, J. E. Kunzler, and F. S. L. Hsu, Phys. Rev. B 1, 366 (1970).

[5]R. D. Parker and M. H. Halloran, Phys. Rev. B 9, 4130 (1974).

[6]R. A. Phillips, Phys. Lett. A36, 361 (1971).

[7]G. B. Scott, M. Springford, and J. R. Stockton, Phys. Lett. 27A, 655 (1968).

[8]L. F. Mattheiss, Phys. Rev. B 1, 373 (1970).

[9]J. C. Slater, Phys. Rev. 81, 385 (1951).

[10]W. Kohn and L. J. Sham. Phys. Rev. 140, A1133 (1965).

[11]R. Gáspár, Acta Phys. Hung. 3, 264 (1954).

[12]D. A. Papaconstantopoulos, J. R. Anderson, and J. W. McCaffrey, Phys. Rev. B 5, 1214 (1972).

[13]J. R. Anderson, D. A. Papaconstantopoulos, J. W. McCaffrey, and J. E. Schirber, Phys. Rev. B 7, 5115 (1973).

[14]S. Wakoh, Y. Kubo, and J. Yamashita, J. Phys. Soc. Jpn. 38, 416 (1975).

[15]S. Wakoh and J. Yamashita, J. Phys. Soc. Jpn. 35, 1394 (1973).

[16]In the $X\alpha$ method the value of α is taken to be that for which the Hartree-Fock-Slater total energy of the atom is the same as the Hartree-Fock energy. These values have been determined by K. Schwarz, Phys. Rev. B 5, 2466 (1972); and Theor. Chim. Acta 34, 225 (1974).

[17]L. Hedin and B. I. Lundqvist, J. Phys. C 4, 2064 (1971).

[18]V. L. Moruzzi, J. F. Janak, and A. R. Williams, Bull. Am. Phys. Soc. 21, 307 (1976).

[19]G. S. Painter, J. S. Faulkner, and G. M. Stocks, Phys. Rev. B 9, 2448 (1974).

[20]N. Elyashar and D. D. Koelling, Phys. Rev. B 13, 5362 (1976); and private communication.

[21]L. L. Boyer and B. M. Klein, Int. J. Quantum Chem. S9, 511 (1975).

[22]J. C. Slater and G. F. Koster, Phys. Rev. 94, 1498 (1954).

[23]F. M. Mueller, J. W. Garland, M. H. Cohen, and K. H. Bennemann, Ann. Phys. (N.Y.) 67, 19 (1971).

[24]A. R. Williams, V. L. Moruzzi, and J. F. Janak (unpublished).

[25]W. L. McMillan, Phys. Rev. 163, 331 (1968).

[26]L. L. Boyer, B. M. Klein, and D. A. Papaconstantopoulos, Ferroelectrics (to be published).

[27]G. D. Gaspari and B. L. Gyorffy, Phys. Rev. Lett. 28, 801 (1972).

[28]W. H. Butler and P. B. Allen, in *Proceedings of the Second Rochester Conference on Superconductivity of d- and f-Band Metals*, edited by D. H. Douglas, Jr. (Plenum, New York, 1976) pp. 73–120.